

## MODELING FREQUENCY-DEPENDENT SELECTION WITH AN APPLICATION TO CICHLID FISH

SHEREE L. ARPIN\* AND J. M. CUSHING\*#

Interdisciplinary Program in Applied Mathematics\*

Department of Mathematics#

617 N Santa Rita

University of Arizona, Tucson AZ 85721, USA

**ABSTRACT.** Negative frequency-dependent selection is a well known microevolutionary process that has been documented in a population of *Perissodus microlepis*, a species of cichlid fish endemic to Lake Tanganyika (Africa). Adult *P. microlepis* are lepidophages, feeding on the scales of other living fish. As an adaptation for this feeding behavior *P. microlepis* exhibit lateral asymmetry with respect to jaw morphology: the mouth either opens to the right or left side of the body. Field data illustrate a temporal phenotypic oscillation in the mouth-handedness, and this oscillation is maintained by frequency-dependent selection. Since both genetic and population dynamics occur on the same time scale in this case, we develop a (discrete time) model for *P. microlepis* populations that accounts for both dynamic processes. We establish conditions on model parameters under which the model predicts extinction and conditions under which there exists a unique positive (survival) equilibrium. We show that at the positive equilibrium there is a 1:1 phenotypic ratio. Using a local stability and bifurcation analysis, we give further conditions under which the positive equilibrium is stable and conditions under which it is unstable. Destabilization results in a bifurcation to a periodic oscillation and occurs when frequency-dependent selection is sufficiently strong. This bifurcation is offered as an explanation of the phenotypic frequency oscillations observed in *P. microlepis*. An analysis of the bifurcating periodic cycle results in some interesting and unexpected predictions.

**1. Introduction.** Frequency-dependent selection (FDS) is a form of natural selection where the fitness of a genotype depends on the frequency of that genotype in a population [9]. Numerous laboratory studies have shown that FDS operates in a plethora of organisms: *Drosophila*, *Tribolium*, houseflies, butterflies, wheat, barley, grass, flowering plants, water boatmen, guppies, house wrens, and mice [3], [8], [9], [10]. While FDS was well-documented in laboratory populations, convincing evidence of its occurrence in the field was noticeably absent [3] until 1993 when M. Hori reported FDS operating in a natural population of predatory cichlid fish (*Perissodus microlepis* Boulenger) [11].

The type of FDS that Hori documented is called negative FDS. Negative FDS occurs when the fitness of a genotype is a *decreasing* function of genotypic frequency in a population. That is, individuals with *rare* genotypes have *greater* fitness than

---

2000 *Mathematics Subject Classification.* Primary: 92D40, 92D25, 92D10; Secondary: 39A11.

*Key words and phrases.* population dynamics, population genetics, frequency-dependent selection, microevolution, phenotypic oscillation period doubling bifurcation.

Authors supported in part by NSF grant DMS-0414142.

individuals with common genotypes. Negative FDS is of special interest as an evolutionary force because it leads to balanced polymorphism (genetic diversity). The amount of genetic diversity a population possesses dictates the evolutionary potential of the population, since existing genetic variation is required for adaptation. Early experimental evidence of negative FDS selection dates back to 1946 laboratory studies of karyotypes in *Drosophila pseudoobscura* [18]. Negative FDS has also been found to operate on pathogen resistance genes, predator-prey systems using search images, self-incompatibility loci in plants, species competing for limited resources, and mating preferences (i.e., frequency-dependent sexual selection) [2], [4], [7], [13], [16].

To understand why *P. microlepis* is subject to negative FDS we need to know a few basic facts about the species' biology and ecology. *P. microlepis* attack their prey from behind and use their spine-like teeth to remove scales. Prey fish are keenly alert to approaching predators, and the rate of hunting success is low, approximately 20% [11]. Interestingly, Hori discovered that *P. microlepis* possess a lateral jaw asymmetry; there is an asymmetrical joint of the jaw to the suspensorium [12]. Populations of *P. microlepis* are polymorphic with respect to jaw morphology; an individual's jaw either opens to the left (sinistral) side or to the right (dextral) side of the body. No intermediate forms have been observed. Hori discovered that left-handed (sinistral) fish consistently attack the prey's right flank and right-handed (dextral) fish consistently attack the prey's left flank. This behavior appears to be adaptive by increasing the contact area between the jaw and the prey's body [11]. Prey fish are sensitive to the number of attacks received on each flank (a function of the number of individuals possessing each phenotype) and respond by guarding the heavily targeted side more aggressively. This behavior, in turn, gives the fish possessing the opposite morphology a hunting advantage. The hunting advantage translates into marked differences in reproductive output. In fact, field data indicate that the rare type can have twice the reproductive success of the common type [17]. Collectively, the data, observations, and experiments indicate that jaw polymorphism for *P. microlepis* is maintained by negative FDS, which is mediated by the guarding behavior of the prey fish.

Beside documenting the occurrence of negative FDS in a field study, Hori made another intriguing discovery. Data collected over more than eleven years showed that phenotypic frequencies did not stabilize, but instead exhibited an oscillation on a relatively short time scale (roughly 5 years). In an attempt to explain this oscillation Takahashi and Hori [17] utilize a discrete-time population genetic model of frequency-dependent selection and argue that a polymorphic equilibrium corresponding to a 1:1 phenotypic ratio can be destabilized when frequency-dependent selection is sufficiently strong. They also attribute the phenotypic oscillation, in part, to a time lag caused by the juvenile growth period. (All other analysis for *P. microlepis* carried in [17] utilized a haploid model.) Their model is not without some weaknesses, however. These include the difficulty in describing transitions from one generation to the next for a species (like *P. microlepis*) with overlapping generations by a model that uses frequencies as its state variables. Furthermore, the authors' consider only population genetic processes despite the short evolutionary time scale. Motivated by Takahashi and Hori's approach and intriguing findings we investigate a modified and extended population/genetic model for the population/genetic dynamics of negative FDS. We will show how our model corroborates the basic conclusions of Takahashi and Hori concerning the cause of destabilization

and oscillation. We will not investigate the role of juvenile development in the form of stage-structure in this paper, however. This is done by extensions of the model presented here in [1]. We also do not consider predator-prey dynamics in our model; interesting predator-prey models for *P. microlepis* are investigated in [14], [15].

With rare exceptions population genetic models ignore the fundamental processes of population dynamic models, and vice versa. Population dynamic models typically overlook variation among genotypes, and population genetic models typically overlook demographic processes such as births, deaths and intraspecific competition occurring on a short time scale. These simplifications are usually justified by differences in ecological and evolutionary time scales, the former being considerably shorter than the latter. On the other hand, the modeling of microevolution (roughly defined as changes in allele frequencies in a population over relatively short time scales) necessitates the consideration of both population dynamic and population genetic processes.

Handedness in *P. microlepis* is heritable and determined by a simple Mendelian one-locus, two-allele mode of inheritance where dextrality is completely dominant over sinistrality; heterozygous and homozygous right-handed individuals are phenotypically indistinguishable [11]. The state variables in our model are absolute numbers of *P. microlepis* comprising each genotype. In this way we can accurately account for overlapping generations and examine reproductive success and selection at the level of mate pairing without assuming individual fertilities are independent of one another. We avoid the typical case that viabilities and fertilities are assigned to individuals possessing each genotype irrespective of mate pairings that form. Instead, we assume that the fertility of a mate pairing is a function of the fitness of the individuals comprising the mating pair, a key point since differential reproductive success is what can give rise to phenotypic oscillations. Furthermore, we are interested in exploiting the relatively simple genetics of *P. microlepis* in order to investigate the interplay between the population genetic and population dynamic processes. We aspire towards a level of mathematical rigor and generality so that the model can be applied to other biological systems with similar genetic constraints.

**2. Model Construction.** We construct a system of three difference equations that predict the numbers of sexually mature, scale-eating adult fish of each handed genotype at time  $t + 1$  from the numbers present at time  $t$ . While this model will not provide a dynamical system for genotype frequencies, one can straightforwardly calculate these frequencies at each time from model state variables. In this way the model accounts for both population dynamics and phenotypic frequency dynamics. The projection time interval for the model is two years: the approximate time from birth to sexual maturity and scale-eating in *P. microlepis*. In this paper we will purposefully utilize a “weak” density-dependent nonlinearity so as to avoid oscillations due to strong intraspecific competition in the population dynamics. In this way, we can focus on oscillations caused by the genetic processes, as opposed to population dynamic processes.

We define the model state variables  $A_{LL}(t)$ ,  $A_{RL}(t)$ , and  $A_{RR}(t)$  to be respectively the numbers of (homozygous) left-handed, heterozygous right-handed, and homozygous right-handed sexually mature, scale-eating adult fish at time  $t$ . Let  $N(t) = A_{LL}(t) + A_{RL}(t) + A_{RR}(t)$  denote the total population size at time  $t$ . If  $n$  denotes the expected number of matings per adult (per unit time) and  $b$  the inherent

number of offspring per mating (i.e., the expected number of offspring possible per mating in the absence of population density effects), then the total number of matings at time  $t$  would be  $nbN(t)$ . We assume, however, that the density dependent total number of matings is

$$\frac{nbN(t)}{1 + cN(t)}$$

for a positive constant  $c > 0$ . This is the familiar Beverton-Holt assumption that typically gives rise to logistic type population dynamics. In order to determine the state variables at time  $t + 1$ , under the assumption of random mating, we need to account for the proportions of each genotypic type of offspring that result from various genotypic mating pairs. We will illustrate this bookkeeping for  $A_{LL}(t + 1)$ ; the derivations for the other two state variables are similar.

Mating is assumed to be random, and we do not distinguish between the matings  $A_{RR}$  (male)  $\times$   $A_{RL}$  (female) and  $A_{RR}$  (female)  $\times$   $A_{RL}$  (male), for example. We assume there is an equal sex ratio and that both sexes have identical allele frequencies. The genotypic frequencies at each time are determined by the following ratios:

$$\frac{A_{LL}(t)}{N(t)}, \quad \frac{A_{RL}(t)}{N(t)}, \quad \frac{A_{RR}(t)}{N(t)}.$$

The phenotypic frequencies of left-handed and right-handed fish at time  $t$  are respectively

$$l(t) \triangleq \frac{A_{LL}(t)}{N(t)}, \quad 1 - l(t) = \frac{A_{RL}(t) + A_{RR}(t)}{N(t)}$$

since the dextral allele ( $R$ ) is completely dominant over the sinistral allele ( $L$ ). In the absence of selection and genetic drift the probability that a mating event will produce an offspring with a particular genotype can be determined by the Hardy-Weinberg Law. Hardy-Weinberg equilibrium cannot be reached in the case of *P. microlepis*, however, because the assumption that there is no selection is violated.

The fraction of all mate pairings that involve only left-handed adults, under the assumption of random mating, is potentially  $l^2(t)$ . We assume a fraction  $f_1$  of this potential fraction consists of successful matings. Therefore, of all matings that occur, the fraction that occurs between left-handed adults is  $l^2(t)f_1$ . In order to account for frequency-dependent selection, we assume  $f_1$  is a function of the phenotypic frequency, i.e., we assume  $f_1 = f_1(l(t))$  and call the function  $f_1(\cdot)$  the *fitness function for matings between phenotypically alike adults*. This assumption implicitly models the guarding behavior of the prey species, which is dependent on phenotypic frequencies. Since this guarding behavior favors the rare phenotype, resulting in negative frequency-dependent selection, we assume  $f_1(l)$  is a decreasing function of  $l$ . Further assumptions on the function  $f_1(l)$  appear below. (Although we know frequency-dependent selection operates in populations of *P. microlepis*, we do not specify the particular type of selection, e.g., viability selection, mating success, fecundity selection). Using this notation, we calculate the contribution to the number of phenotypically left-handed adults  $A_{LL}(t + 1)$  from matings between left-handed adults to be

$$\frac{nbN(t)}{1 + cN(t)} \left( \frac{A_{LL}(t)}{N(t)} \right)^2 f_1 \left( \frac{A_{LL}(t)}{N(t)} \right). \quad (1)$$

Left-handed offspring can also result from two other types of matings. Specifically, they can result (a) from matings between left-handed and heterozygous right-handed adults and (b) from two heterozygous right-handed adults. In case (b) we

calculate, using the reasoning and notation above, the contribution to the number of phenotypically left-handed adults  $A_{LL}(t + 1)$  from such matings to be

$$\frac{nbN(t)}{1 + cN(t)} \frac{1}{4} \left( \frac{A_{RL}(t)}{N(t)} \right)^2 f_1 \left( 1 - \frac{A_{LL}(t)}{N(t)} \right). \tag{2}$$

The reason for the factor 1/4 is that only one quarter of all matings between two heterozygous right-handed adults will be left-handed (because the dextral allele is completely dominant over the sinistral allele). Notice that the fitness of these mate pairings is (due to the negative-frequency dependent selection caused by the guarding behavior of the prey) a decreasing function of the frequency of *right*-handed fish. In case (a) we calculate, in a similar manner, the contribution to the number of phenotypically left-handed adults  $A_{LL}(t + 1)$  to be

$$\frac{nbN(t)}{1 + cN(t)} \left( \frac{1}{2} \frac{A_{LL}(t)}{N(t)} \frac{A_{RL}(t)}{N(t)} + \frac{1}{2} \frac{A_{RL}(t)}{N(t)} \frac{A_{LL}(t)}{N(t)} \right) f_2 \left( \frac{A_{LL}(t)}{N(t)} \right). \tag{3}$$

Half the matings of type  $A_{RR}$  (male)  $\times$   $A_{RL}$  (female) and half the matings of type  $A_{RR}$  (female)  $\times$   $A_{RL}$  (male) are left-handed. Assumptions about the *fitness function*  $f_2(\cdot)$  for matings between phenotypically different adults appear below.

The number of left-handed fish  $A_{LL}(t + 1)$  at time  $t + 1$  consists of the total of all recruits obtained from the sum of (1-3) plus all surviving left-handed adults, which we assume is  $(1 - \mu_a)A_{LL}(t)$ . Thus,

$$A_{LL}(t + 1) = \frac{nbN(t)}{1 + cN(t)} \left[ \left( \frac{A_{LL}(t)}{N(t)} \right)^2 f_1 \left( \frac{A_{LL}(t)}{N(t)} \right) + \frac{A_{LL}(t)A_{RL}(t)}{N^2(t)} f_2 \left( \frac{A_{LL}(t)}{N(t)} \right) + \frac{1}{4} \left( \frac{A_{RL}(t)}{N(t)} \right)^2 f_1 \left( 1 - \frac{A_{LL}(t)}{N(t)} \right) \right] + (1 - \mu_a) A_{LL}(t). \tag{4}$$

By constructing our model with absolute numbers as state variables, we can assign a fitness to the various mate pairings based on the individual phenotypes comprising the pair. Modeling allele or genotype frequencies does not make it possible to assign fitness values to mating pairs. This is especially problematic when the reproductive success of a mating between individuals possessing different phenotypes is resolved by the more fit (or less fit) individual in the pairing. Maximal reproductive success  $b$  is reduced by the frequency-dependent fitness functions  $f_1$  and  $f_2$  in accordance with the phenotypic frequencies. The number of offspring produced per mating is reduced when ideal conditions (i.e., when  $A_{LL}(t) / (A_{RL}(t) + A_{RR}(t)) \approx 0$  or  $(A_{RL}(t) + A_{RR}(t)) / A_{LL}(t) \approx 0$ ) are not met. The inequalities  $0 \leq f_i(l) \leq 1$  describe the fact that reproductive success is reduced by frequency-dependent selection. Since the phenotypic fitness are equal when the phenotypic ratio is 1:1, we have  $f_1(1/2) = f_2(1/2)$ .

Repeating similar derivation steps for  $A_{RL}(t+1)$ , and  $A_{RR}(t+1)$ , we arrive at the equations

$$\begin{aligned}
 A_{LL}(t+1) &= \frac{nbN(t)}{1+cN(t)} \left[ \left( \frac{A_{LL}(t)}{N(t)} \right)^2 f_1 \left( \frac{A_{LL}(t)}{N(t)} \right) + \frac{A_{LL}(t)A_{RL}(t)}{N^2(t)} f_2 \left( \frac{A_{LL}(t)}{N(t)} \right) \right. \\
 &\quad \left. + \frac{1}{4} \left( \frac{A_{RL}(t)}{N(t)} \right)^2 f_1 \left( 1 - \frac{A_{LL}(t)}{N(t)} \right) \right] + (1 - \mu_a) A_{LL}(t) \\
 A_{RL}(t+1) &= \frac{nbN(t)}{1+cN(t)} \left[ \frac{\frac{1}{2}A_{RL}^2(t) + A_{RR}(t)A_{RL}(t)}{N^2(t)} f_1 \left( 1 - \frac{A_{LL}(t)}{N(t)} \right) \right. \\
 &\quad \left. + \frac{A_{LL}(t)A_{RL}(t) + 2A_{RR}(t)A_{LL}(t)}{N^2(t)} f_2 \left( \frac{A_{LL}(t)}{N(t)} \right) \right] \\
 &\quad + (1 - \mu_a) A_{RL}(t) \\
 A_{RR}(t+1) &= \frac{nbN(t)}{1+cN(t)} \left[ \frac{A_{RR}^2(t) + A_{RR}(t)A_{RL}(t) + \frac{1}{4}A_{RL}^2(t)}{N^2(t)} \right] f_1 \left( 1 - \frac{A_{LL}(t)}{N(t)} \right) \\
 &\quad + (1 - \mu_a) A_{RR}(t).
 \end{aligned} \tag{5}$$

We will study these model equations under the following assumptions:

$$n, b, c > 0, \quad 0 < \mu_a < 1 \tag{6a}$$

$$f_i \in C^1([0, 1] \rightarrow [0, 1]), \quad f_1(1/2) = f_2(1/2) \tag{6b}$$

$$\frac{df_1}{dl} < 0, \quad \frac{df_1}{dl} \Big|_{l=x} = \frac{df_1}{dl} \Big|_{l=1-x} \tag{6c}$$

$$\min\{f_1(l), f_1(1-l)\} \leq f_2(l) \leq \max\{f_1(l), f_1(1-l)\} \tag{6d}$$

$$f_2(l) = f_2(1-l). \tag{6e}$$

Following the model presented in [17], we assume in (6a) that the probability of death in one time-step,  $\mu_a$ , is density- and frequency-independent. This assumption is supported biologically, in part, by the evidence that selection acts through differential reproductive success as opposed to differential survival. The monotonicity assumption (6c) on  $f_1$  reflects the negative frequency-dependent selection on phenotypic handedness. The symmetry condition on the derivative of  $f_1$  is mathematically equivalent to

$$f_1 \left( \frac{1}{2} - x \right) - f_1 \left( \frac{1}{2} \right) = f_1 \left( \frac{1}{2} \right) - f_1 \left( \frac{1}{2} + x \right),$$

which means that, when a deviation from the 1:1 phenotypic ratio occurs, the *increase* in fitness enjoyed by the rare type is equal in magnitude to the *decrease* in fitness suffered by the common type. The bounds placed on  $f_2$  in (6d) are a result of the fact that matings between individuals possessing different phenotypes are comprised of one individual that is less fit than its mate. The inequalities mean that the less (more) fit mate confers a lower (higher) fitness than would occur in a mating of individuals of the same fitness. Finally, the symmetry condition (6e) on  $f_2$  (which, along with (6b), implies  $f_2'(1/2) = 0$ ) is the result of assuming that the fitness of matings between individuals with different phenotypes is not dependent on which of the phenotypes is the more common. Although we do not mathematically need it, a reasonable biologically assumption would be that  $f_2(l)$  is monotone for  $l < 1/2$  and also for  $l > 1/2$ . See Figure 1.

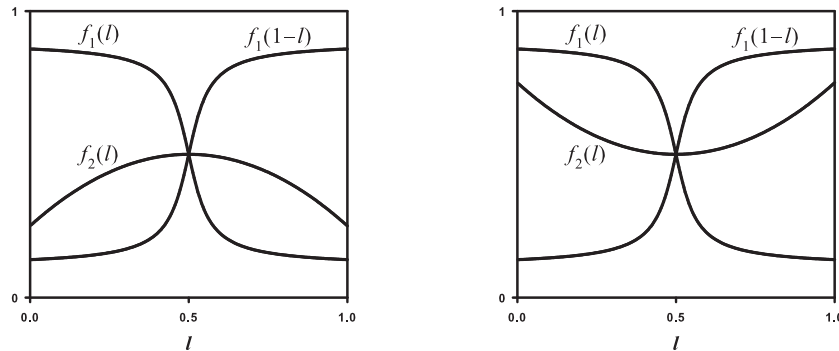


Figure 1. Plots of fitness functions satisfying assumptions (6a)-(6e).

Notice that assumptions (6a) and (6b) imply that (5) holds the interior  $int(R^3)$  of the positive cone in  $R^3$  invariant, i.e.

$$(A_{LL}(0), A_{RL}(0), A_{RR}(0)) \in int(R^3) \implies (A_{LL}(t), A_{RL}(t), A_{RR}(t)) \in int(R^3)$$

for all  $t = 0, 1, 2, \dots$ . We begin by giving conditions under which a population whose dynamics are governed by (5) goes extinct. The model equations are not defined at the origin  $(A_{LL}, A_{RL}, A_{RR}) = (0, 0, 0)$ . However, it is possible for orbits in  $int(R^3)$  to approach the origin asymptotically.

**Theorem 2.1.** *Assume (6a) and (6b). If  $nb/\mu_a < 1$  then  $\lim_{t \rightarrow +\infty} N(t) = 0$  for any initial condition  $(A_{LL}(0), A_{RL}(0), A_{RR}(0)) \in int(R^3)$ .*

*Proof.* Summing the three equations in (5), we find that

$$N(t+1) = \frac{nbN(t)}{1 + cN(t)} [l^2(t)f_1(l(t)) + 2l(t)(1-l(t))f_2(l(t)) + (1-l(t))^2 f_1(1-l(t))] + (1-\mu_a)N(t)$$

and from (6b) that

$$N(t+1) \leq nbN(t) [l^2(t) + 2l(t)(1-l(t)) + (1-l(t))^2] + (1-\mu_a)N(t) = nbN(t) + (1-\mu_a)N(t).$$

Therefore,  $0 \leq N(t+1) \leq \rho N(t)$  where  $\rho \triangleq nb + 1 - \mu_a$ . Since  $nb/\mu_a < 1$  implies  $\rho < 1$ , it follows that  $\lim_{t \rightarrow +\infty} N(t) = 0$  under this condition.  $\square$

The product  $nb$  is the number of offspring per adult under maximal fitness  $f_i = 1$  (for any genotypic mating pairs). We can therefore interpret the quantity  $nb/\mu_a$  as the maximal inherent net reproductive number for the population, i.e. the expected number of offspring per adult per lifetime (for any mating pair) under conditions of maximal fitness and in the absence of population density effects. Theorem 2.1 asserts the logical conclusion that if this maximal inherent net reproductive number is less than one (i.e., no adult, under any mating conditions and at low population densities, can replace itself during its lifetime) then the population will go extinct.

**3. Polymorphic Equilibria.** Because of the singularity at the origin in model (5), we cannot apply general bifurcation theorems to deduce the existence and stability of nontrivial equilibria [6]. Therefore, we must approach the existence and stability of nontrivial equilibria in another way. The next theorem deals with the existence of polymorphic equilibria, i.e., equilibria that lie on the interior  $int(R^3)$  of the positive cone in  $R^3$ . Define  $R_0 \triangleq nbf(1/2)/\mu_a$ . This quantity is the expected number of offspring per adult (per lifetime) when population density is low and the population is at a 1:1 phenotypic ratio.

**Theorem 3.1.** *Assume (6a)-(6e). If  $R_0 > 1$  model (5) has a unique polymorphic equilibrium given by*

$$(A_{LL}^*, A_{RL}^*, A_{RR}^*) \triangleq N^* \left( \frac{1}{2}, \sqrt{2} - 1, \frac{3}{2} - \sqrt{2} \right) \tag{7}$$

where

$$N^* = A_{LL}^* + A_{RL}^* + A_{RR}^* = \frac{R_0 - 1}{c}$$

is the total population size at equilibrium. Notice that at this equilibrium left- and right-handed phenotypes are equally frequent.

This theorem implies the existence of a polymorphic equilibrium if, under the conditions of a 1:1 phenotypic ratio and no population density effects, an adult will more than replace itself during its lifetime. Moreover, the theorem asserts that at this equilibrium there will in fact be a 1:1 phenotypic ratio. The existence of such an equilibrium corroborates the conclusion of Takahashi and Hori [17]. Furthermore, we have shown that this is the only polymorphic equilibrium.

*Proof.* A straightforward, but tedious, calculation shows that the triple (7) is an equilibrium of (5). It is left to show that (7) is the only polymorphic equilibrium. Let  $(A'_{LL}, A'_{RL}, A'_{RR}) \in int(R^3)$  be an equilibrium of (5) and let

$$N' = A'_{LL} + A'_{RL} + A'_{RR}, \quad \alpha \triangleq \frac{A'_{LL}}{N'}, \quad \beta \triangleq \frac{A'_{RL}}{N'}$$

Summing the three equations of model (5) evaluated at the equilibrium we obtain, after the cancellation of a factor of  $N'$  and some algebraic manipulations, the equation

$$\frac{1}{1 + cN'} = \frac{\mu_a}{nb \left( \alpha^2 f_1(\alpha) + 2\alpha(1 - \alpha) f_2(\alpha) + (1 - \alpha)^2 f_1(1 - \alpha) \right)}. \tag{8}$$

A substitution of  $\alpha, \beta$ , and  $1 - \alpha - \beta = A'_{RR}/N'$  into the three equilibrium equations of (5) yields

$$\begin{aligned} \mu_a \alpha &= \frac{nB}{1 + cN'} \left[ \alpha^2 f_1(\alpha) + \alpha\beta f_2(\alpha) + \beta^2 f_1(1 - \alpha) / 4 \right] \\ \mu_a \beta &= \frac{nB}{1 + cN'} \left[ (\beta^2 / 2 + (1 - \alpha - \beta)\beta) f_1(1 - \alpha) \right. \\ &\quad \left. + (\alpha\beta + 2(1 - \alpha - \beta)\alpha) f_2(\alpha) \right] \\ \mu_a (1 - \alpha - \beta) &= \frac{nB}{1 + cN'} \left( (1 - \alpha - \beta)^2 + (1 - \alpha - \beta)\beta + \beta^2 / 4 \right) f_1(1 - \alpha). \end{aligned}$$

Substitution of (8) into these equations yields the following three quadratic equations in  $\beta$ :

$$\begin{aligned}
 0 &= \beta^2 + \frac{4\alpha f_2(\alpha)}{f_1(1-\alpha)}\beta \\
 &\quad + \frac{4\alpha}{f_1(1-\alpha)} [\alpha(1-\alpha)f_1(\alpha) - 2\alpha(1-\alpha)f_2(\alpha) - (1-\alpha)^2 f_1(1-\alpha)] \\
 0 &= \beta^2 + 2\alpha \frac{\alpha f_1(\alpha) + (3-2\alpha)f_2(\alpha) - (1-\alpha)f_1(1-\alpha)}{f_1(1-\alpha)}\beta - \frac{4\alpha(1-\alpha)f_2(\alpha)}{f_1(1-\alpha)} \\
 0 &= \beta^2 + 4\alpha \frac{\alpha f_1(\alpha) + 2(1-\alpha)f_2(\alpha) - (1-\alpha)f_1(1-\alpha)}{f_1(1-\alpha)}\beta \\
 &\quad - 4\alpha \frac{\alpha(1-\alpha)f_1(\alpha) + 2(1-\alpha)^2 f_2(\alpha) - (1-\alpha)^2 f_1(1-\alpha)}{f_1(1-\alpha)}.
 \end{aligned}$$

We solve each equation for  $\beta$  and we require that the results be equal. This calculation (done with the aid of a computer algebra program) results in the equation

$$G(\alpha) \triangleq \alpha f_1(\alpha) + (1-2\alpha)f_2(\alpha) - (1-\alpha)f_1(1-\alpha) = 0.$$

for  $\alpha$ . Clearly,  $\alpha = 1/2$  solves this equation; our next goal is to show that this is the only solution.

Suppose  $\alpha > 1/2$ . Then by (6d) we have  $f_2(\alpha) \geq \min\{f_1(\alpha), f_1(1-\alpha)\} = f_1(\alpha)$ . It follows that

$$G(\alpha) \leq \alpha f_1(\alpha) + (1-2\alpha)f_1(\alpha) - (1-\alpha)f_1(1-\alpha) = (1-\alpha)[f_1(\alpha) - f_1(1-\alpha)] < 0$$

and hence  $G(\alpha)$  has no root  $\alpha > 1/2$ . Suppose, on the other hand that,  $\alpha < 1/2$ . Then by (6d) we have  $f_2(\alpha) \geq \min\{f_1(\alpha), f_1(1-\alpha)\} = f_1(1-\alpha)$ . It follows that

$$G(\alpha) \geq \alpha f_1(\alpha) + (1-2\alpha)f_1(1-\alpha) - (1-\alpha)f_1(1-\alpha) = \alpha[f_1(\alpha) - f_1(1-\alpha)] > 0$$

and hence  $G(\alpha)$  has no root  $\alpha < 1/2$ . This proves that

$$\alpha = \frac{A'_{LL}}{N'} = \frac{1}{2}, \quad 1-\alpha = \frac{A'_{RL} + A'_{RR}}{N'} = \frac{1}{2} \tag{9}$$

for any equilibrium in  $int(R^3)$ .

Clearly there are infinitely many triples  $(A'_{LL}, A'_{RL}, A'_{RR})$  that satisfy (9). However, all three of the quadratic equations (in  $\beta$ ) with  $\alpha = 1/2$  reduce to  $\beta^2 + 2\beta - 1 = 0$ , and we conclude that

$$\beta = \frac{A'_{RL}}{N'} = \sqrt{2} - 1. \tag{10}$$

If we solve equation (8) for  $N'$  with  $\alpha = 1/2$ , we find that  $N' = N^*$ . This result, together with the formulas (9) and (10), show  $(A'_{LL}, A'_{LR}, A'_{RR})$  is equal to the equilibrium (7).  $\square$

We now turn attention to the local stability of the polymorphic equilibrium in Theorem 3.1. By taking advantage of the formula for the polymorphic equilibrium (7) and the fact that (6b) and (6e) imply  $f'_2(1/2) = 0$ , we calculate the eigenvalues of the Jacobian of (5) at this equilibrium to be

$$\begin{aligned}
 \lambda_1 &= 1 - \mu_a, \quad \lambda_2 = \frac{R_0(1-\mu_a) + \mu_a}{R_0} = 1 + \frac{1-R_0}{R_0} \mu_a \\
 \lambda_3 &= 1 + \frac{\sqrt{2}-1}{2} \mu_a \frac{f'_1(1/2)}{f_1(1/2)}.
 \end{aligned}$$

Assumptions (6a)-(6e), together with  $R_0 > 1$  in Theorem 3.1, imply that  $0 < \lambda_1, \lambda_2 < 1$  and consequently the local stability of (7) depends on  $\lambda_3$ . Since  $f'_1(1/2) < 0$  by (6c) it follows that  $\lambda_3 < 1$ . By the linearization principle, the polymorphic equilibrium (7) is locally stable if  $\lambda_3 > -1$  and unstable if  $\lambda_3 < -1$ . Define

$$q \triangleq f'_1(1/2) < 0, \quad q_{cr} \triangleq -\frac{4f_1(1/2)/\mu_a}{\sqrt{2}-1} < 0.$$

**Theorem 3.2.** *Assume (6a)-(6e) and  $R_0 > 1$ . The polymorphic equilibrium (7) in Theorem 3.1 is locally asymptotically stable if  $q > q_{cr}$  and unstable if  $q < q_{cr}$ .*

The quantity  $q$  (similarly defined by Takahashi and Hori [17]) is a critical quantity for determining the stability and the destabilization of the polymorphic equilibrium. Recall that  $f_1(l)$  and  $f_1(1-l)$  determine the fitness of matings between like phenotypes (namely, left-handed with left-handed matings and right-handed with right-handed matings respectively). The magnitude of  $q$  determines the extent to which small deviations from a 1:1 phenotypic ratio translate to changes in the fitness of matings between like phenotypes. If  $|q|$  is large, a small departure from a 1:1 phenotypic ratio results in a large difference in reproductive success. On the other hand, matings between unlike phenotypes, accounted for by the function  $f_2$ , do not alter the stability of the polymorphic equilibrium. In particular, recall that under our assumptions  $f'_2(1/2) = 0$ ; this implies that small deviations from a 1:1 phenotypic ratio cannot drastically affect the reproductive success of mate pairings between unlike phenotypes.

**4. Periodic Oscillations.** Since  $\lambda_3 = -1$  when  $q = q_{cr}$ , Theorem 3.2 suggests the occurrence of a period doubling bifurcation at this value of  $q$ . Mathematically, we can investigate the properties (and prove the existence) of the bifurcating 2-cycles, at least near the bifurcation point, by classical Lyapunov-Schmidt methods [6]. Since this calculation is straightforward (albeit tedious), we will not give the details here, but instead describe the results only. For  $q \gtrsim q_{cr}$  the 2-cycles are approximated by

$$\begin{aligned} A_{LL}(t) &= \frac{1}{2}N^* + (\sqrt{2} + 1)(-1)^t\varepsilon + x^*\varepsilon^2 + O(\varepsilon^3) \\ A_{RL}(t) &= (\sqrt{2} - 1)N^* - \sqrt{2}(-1)^t\varepsilon + y^*\varepsilon^2 + O(\varepsilon^3) \\ A_{RR}(t) &= \left(\frac{3}{2} - \sqrt{2}\right)N^* - (-1)^t\varepsilon + z^*\varepsilon^2 + O(\varepsilon^3) \end{aligned} \tag{11}$$

for  $\varepsilon \gtrsim 0$  where  $\varepsilon$  is proportional to  $(q - q_{cr})^{1/2}$  and where  $x^*$ ,  $y^*$ , and  $z^*$  turn out to be constants. From these we calculate an expansion for the total numbers of right-handed phenotypes:

$$A_{RL}(t) + A_{RR}(t) = \frac{1}{2}N^* - (\sqrt{2} + 1)(-1)^t\varepsilon + (y^* + z^*)\varepsilon^2 + O(\varepsilon^3).$$

Notice that, to first order in  $\varepsilon$ , the oscillations in population numbers  $A_{LL}(t)$  and  $A_{RL}(t) + A_{RR}(t)$  of the left- and of the right-handed are of equal magnitude, but out-of-phase, around the same average  $N^*/2$ . Thus on average, over the 2-cycle, they bear a 1:1 ratio. However, to second order in  $\varepsilon$  there are adjustments to these averages since the coefficients  $x^*$ ,  $y^*$ , and  $z^*$  are constants. Formulas for these

coefficients appear in [1]; they are quite complicated and we do not need to repeat them here. It turns out that

$$x^* < 0 \quad \text{and} \quad x^* - (y^* + z^*) = \frac{-k}{bn(\sqrt{2} - 1)q + 4}.$$

for a positive constant  $k > 0$  (dependent only on  $c$ ). If we assume  $R_0 > 1$  (so that there exists a polymorphic equilibrium), then

$$q_{cr} = -\frac{4f_1(1/2)}{\mu_a(\sqrt{2} - 1)} < -\frac{1}{bn} \frac{4}{\sqrt{2} - 1}.$$

As a result, if  $q < q_{cr}$  (so that there exists a bifurcating 2-cycle) then  $0 > x^* > y^* + z^*$ .

It follows that for  $q \lesssim q_{cr}$  the average of the 2-cycle population numbers of the left-handed phenotype is greater than that of the right-handed phenotypes and both are less than the equilibrium level of  $N^*/2$ . Moreover, to second order in  $\varepsilon$  the total population size

$$N(t) = N^* + (x^* + y^* + z^*)\varepsilon^2 + O(\varepsilon^3)$$

is constant. It follows that the (cycle) average phenotypic frequencies are not in a 1:1 ratio; specifically, the average frequency of the left-handed phenotype is greater than the average of the (genetically dominant) right-handed phenotype. The bifurcation diagrams in Figure 2 illustrate these properties of the 2-cycle oscillation for model (5) with

$$nb = 50, \quad c = 0.1, \quad \mu_a = 0.6, \quad f_1(l) \equiv \frac{1}{2} \left( 1 - \tanh \left[ 2q \left( \frac{1}{2} - l \right) \right] \right), \quad f_2(l) \equiv \frac{1}{2}. \quad (12)$$

**Theorem 4.1.** *Assume (6a)-(6e) and  $R_0 > 1$ . For  $q \lesssim q_{cr}$  the bifurcating 2-cycles of (5) are approximated by the expansions (11) for small  $\varepsilon \gtrsim 0$ . These expansions imply that the 2-cycle oscillations have the following properties:*

- (a) *the total number of left-handed phenotypes and of right-handed phenotypes oscillate around their averages with equal amplitudes  $\sqrt{2} + 1$ , but out-of-phase;*
- (b) *the average number of left-handed phenotypes in the 2-cycle and the average number of right-handed phenotypes in the 2-cycle are both less than half the equilibrium levels of  $N^*/2$ ;*
- (c) *the average left-handed phenotypic frequency is greater than 1/2 (and hence that of the right-handed phenotypic frequency is less than 1/2).*

The proof this theorem, being based on the expansions (11), guarantees properties (b) and (c) hold only near the period doubling bifurcation point  $q = q_{cr}$ . Numerical simulations suggest, however, that these properties of the 2-cycle oscillations are not confined near the bifurcation point. In fact, we were not able to find a numerical example where the time-averaged frequency of the right-handed phenotype is greater than the time-averaged frequency of left-handed phenotype.

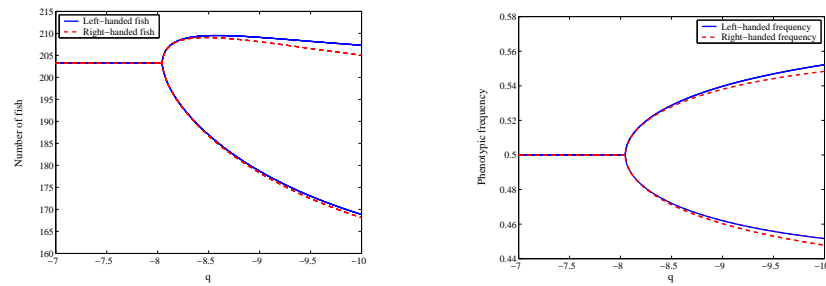


Figure 2. Bifurcation diagrams showing the period doubling bifurcation in model (5) with parameters and fitness functions (12). The left panel shows the number of fish possessing each phenotype and the right panel shows the phenotypic frequencies.

A priori, one might have expected the time-average population numbers or frequencies of the two phenotypes to be equal. Moreover, in the model (5) it is assumed that the allele for the right-handed trait is completely genetically dominant over the allele for the left-handed trait, and therefore it might seem counter-intuitive that the genotype with two recessive alleles is numerically dominant on average. Upon closer consideration, however, this finding might have been expected since a 1 : 1 phenotypic ratio would necessarily force the number of left-handed alleles in the population to be greater than the number of right-handed alleles. In particular, the number of (homozygous) left-handed fish will be greater than the number of homozygous right-handed fish. The number of homozygous fish is critical since matings between like homozygous pairs of a particular phenotype produce 100% homozygous offspring of that phenotype. This fact becomes particularly important when selection is strong: any advantage shared by the rare type can be exploited into a marked differential reproductive success for small deviations from the 1 : 1 phenotypic ratio. For a small, fixed deviation from the 1 : 1 phenotypic ratio, left-handed fish will form a greater number of homozygous mate pairs when rare than will right-handed fish when rare. Furthermore, when the right-handed fish are rare, the left-handed fish gain a reproductive advantage since the  $L$  allele is not exposed to selection in the heterozygous state. Near the bifurcation point and the onset of phenotypic oscillations, the oscillations have small amplitudes and our analysis concerning the difference in averaged phenotypic numbers (or frequencies) are mathematically second order in nature. This means these phenomena might be difficult to observe in observational or experimental data, at least near the bifurcation point.

**5. Monomorphic Equilibria.** There can be no equilibrium  $(A_{LL}, A_{RL}, A_{RR})$  of (5) in which only heterozygous (necessarily right-handed) adults are present. This is because offspring of all three genotypes arise from matings between heterozygous individuals. Model (5) does have, however, two nontrivial equilibria in which only homozygous individuals are present, namely,

$$E_1 \triangleq \left( \frac{nb f_1(1)/\mu_a - 1}{c}, 0, 0 \right), \quad E_2 \triangleq \left( 0, 0, \frac{nb f_1(1)/\mu_a - 1}{c} \right). \quad (13)$$

The monomorphic equilibrium  $E_1$  is characterized by the presence of only left-handed adults (which are necessarily homozygous), while  $E_2$  is characterized by the presence of only homozygous right-handed adults. These equilibria are biologically meaningful and distinct from the origin if and only if  $nbf_1(1)/\mu_a > 1$ . Since  $nbf_1(1)$  is the number of viable offspring in a homozygous population, the quantity  $nbf_1(1)/\mu_a$  is the expected number of offspring per adult per lifetime (in the absence of population density effects), i.e., the inherent reproductive number for a homozygous population [5], [6]. The monomorphic equilibria (13) are biologically feasible (and not identical with the origin) if and only if the net reproductive number of a homozygous population exceeds 1, so that each (homozygous) adult more than replaces itself at low population density.

The  $3 \times 3$  Jacobian matrix of (5), when evaluated at a monomorphic equilibrium  $E_i$ , has three real eigenvalues  $\lambda_i$ . For both  $E_1$  and  $E_2$  it turns out that

$$\lambda_1 = 1 - \mu_a, \quad \lambda_2 = \frac{nbf_1(1)(1 - \mu_a) + \mu_a^2}{nbf_1(1)}.$$

By assumption (6a),  $0 < \lambda_1 < 1$ . It is easy to see that  $0 < \lambda_2 < 1$  when the equilibria are feasible, i.e., when  $nbf_1(1)/\mu_a > 1$ . The third eigenvalue of  $E_2$  is  $\lambda_3 = 1$ . Consequently  $E_2$  is non-hyperbolic and its stability properties remain an open question. The third eigenvalue of the Jacobian at  $E_1$  turns out to be

$$\lambda_3 = \frac{f_1(1)(1 - \mu_a) + f_2(1)\mu_a}{f_1(1)}.$$

By assumptions (6c)-(6e) it follows that  $f_1(1) = \min\{f_1(1), f_1(0)\} \leq f_2(1)$ . This means  $\lambda_3 \geq 1$  and as a result  $E_1$  cannot be hyperbolicly stable. If  $f_1(1) < f_2(1)$  then  $\lambda_3 > 1$  and  $E_1$  is unstable. This strict inequality means that when the population consists of nearly all left-handed adults, a cross mating with a right-handed adult confers a strictly larger fitness. If no such increase in fitness results from a cross mating, i.e. if  $f_1(1) = f_2(1)$ , then  $\lambda_3 = 1$  and  $E_1$  is non-hyperbolic and its stability properties remain an open question.

Although the linearization fails to determine the stability properties of the monomorphic equilibria  $E_1$  and  $E_2$  under assumptions (6a)-(6e), we conjecture that both are unstable. It would be of interest if, under some conditions, this conjecture is false and one or both monomorphic equilibria is an attractor. Because  $nbf(1)/\mu_a > 1$  implies  $R_0 = nbf_1(\frac{1}{2})/\mu_a > 1$ , such conditions would imply the occurrence of multiple (namely, both monomorphic and polymorphic) attractors. We have, however, seen no evidence of such a case in numerical simulations.

**6. Concluding Remarks.** In application of model (5) to *P. microlepis* our findings corroborate one of the basic assertions in [17] concerning the observed phenotypic oscillations in this predatory species of cichlid fish. As did Takahashi and Hori we interpret the quantity  $|q|$  in Theorems 3.2 and 4.1 as a measure of the prey response sensitivity to attacks by *P. microlepis*, which if large enough results in a destabilization of the polymorphic equilibrium (in 1:1 phenotypic ratio). Mathematically, this destabilization results in a period doubling bifurcation to a 2-cycle in which both population numbers and phenotypic frequencies oscillate (out-of-phase). An interesting result of the analysis of this oscillation shows, however, that the average of the oscillations in phenotypic frequencies do not exhibit a 1:1 ratio; in fact, the average of the genetically dominant right-handed phenotype is less 1/2. The formula for the bifurcation value  $q = q_{cr}$  also shows that higher adult death rates

$\mu_a$  contribute to the destabilization of the polymorphic equilibrium. This result suggests that a strongly iteroparous life-cycle (i.e., a high probability of survival) is a stabilizing factor for species such as *P. microlepis* [17].

Our analysis of model (5), which, unlike the model in [17], lacks a developmental time lag in the form of stage-structure, also demonstrates that stage-structure is not necessary for oscillatory behavior. Extensions of model (5) that include juvenile life-cycle stages appear in [1], where destabilization and bifurcations to oscillatory motion (invariant loops and aperiodic oscillations in the state variables) are studied for the resulting higher dimensional models.

Model (5) is based on the Beverton-Holt model for population dynamics which, as a discrete-time model of logistic growth, exhibits monotonic equilibrium dynamics (and hence no periodic oscillations). Model (5) is a straightforward extension of the Beverton-Holt model that incorporates classic Mendelian (one locus, two allele) genetics. The root cause of the oscillations given by Theorem 4.1 is therefore genetic (as opposed to population dynamic) in nature. If the base population dynamic model did allow oscillations, as would be the case for example if the well-known Ricker model were used in place of the Beverton-Holt model, then there arises the possibility of a complicated interplay between oscillations caused, on the one hand, by population dynamics (over compensatory density dependence) and, on the other hand, by genetics (negative frequency-dependent selection). A study of this interplay appears in [1].

#### REFERENCES

- [1] S. L. Arpin, "Using Mathematical Models to Investigate Phenotypic Oscillations in Cichlid Fish: A Case of Frequency-dependent Selection", Ph.D. dissertation, Interdisciplinary Program in Applied Mathematics, University of Arizona, Tucson, 2007.
- [2] F. J. Ayala, *Frequency-dependent mating advantage in Drosophila*, Behavior Genetics **2** (1972), 85-91.
- [3] F. J. Ayala and C. A. Campbell, *Frequency-dependent selection*, Annual Review of Ecology and Systematics, **5** (1974), 115-138.
- [4] B. C. Clarke, *The evidence for apostatic selection*, Heredity, **124** (1969), 347-352.
- [5] J. M. Cushing and Z. Yicang, *The net reproductive value and stability in structured population models*, Natural Resource Modeling, **8** No. 4 (1994), 1-37.
- [6] J. M. Cushing, "An Introduction to Structured Population Dynamics", CBMS-NSF Regional Conference Series in Applied Mathematics, **Vol. 71**, SIAM, Philadelphia, 1998.
- [7] N. Ellstrand and J. Antonovics, *Experimental studies of the evolutionary significance of sexual reproduction. I. A test of the frequency-dependent selection hypothesis*, Evolution, **38** (1984), 103-115.
- [8] R. Frankham, J. D. Ballou, and D. A. Briscoe, "Introduction to Conservation Genetics", Cambridge University Press, Cambridge, 2002.
- [9] D. J. Futuyma, "Evolutionary Biology" (third edition), Sinauer Associates, Sunderland, Massachusetts, 1998.
- [10] P. W. Hedrick, "Genetics of Populations" (third edition), Jones and Bartlett Publishers, Sudbury, Massachusetts, 2005.
- [11] M. Hori, *Frequency-dependent natural selection in the handedness of scale-eating cichlid fish*, Science, **260** (1993), 216-219.
- [12] M. Hori, *Feeding relationships among cichlid fishes in Lake Tanganyika: effects of intra- and interspecific variations of feeding behaviour on their coexistence*, Ecology International Bulletin, **19** (1991), 89-101.
- [13] C. M. Lively and M. F. Dybdahl, *Parasite adaptation to locally common host genotypes*, Nature, **405** (2000), 679-681.
- [14] M. Nakajima, H. Matsuda, and M. Hori, *A population genetic model for lateral dimorphism frequency in fishes*, Population Ecology, **47** (2005), 83-90.

- [15] M. Nakajima, H. Matsuda, and M. Hori, *Persistence and fluctuation of lateral dimorphism in fishes*, *American Naturalist*, **163** (2004), 692–698.
- [16] A. D. Richman and J. R. Kohn, *Learning from rejection: the evolutionary biology of single-locus incompatibility*, *Trends in Ecology & Evolution*, **11** (1996), 497–502.
- [17] S. Takahashi and M. Hori, *Unstable evolutionarily stable strategy and oscillation: a model of lateral asymmetry in scale-eating cichlids*, *The American Naturalist*, **144** (1994), 1001–1020.
- [18] S. Wright and T. Dobzhansky, *Genetics of natural populations. XII. Experimental reproduction of some of the changes caused by natural selection in certain populations of *Drosophila pseudoobscura**, *Genetics*, **31** (1946), 125–156.

Received on January 9, 2008. Accepted on April 4, 2008.

*E-mail address:* sarpin@frc.mass.edu

*E-mail address:* cushing@math.arizona.edu